The crystal structure of saporin SO6 from *Saponaria officinalis* and its interaction with the ribosome

Carmelinda Savino, Luca Federici, Rodolfo Ippoliti, Eugenio Lendaro, Demetrius Tsernoglou*

Department of Biochemical Sciences and CNR Centre for Molecular Biology, University of Rome 'La Sapienza', Piazzale Aldo Moro 5, 00185 Rome, Italy

Received 21 December 1999; received in revised form 21 February 2000

Edited by Richard Cogdell

Abstract The 2.0 Å resolution crystal structure of the ribosome inactivating protein saporin (isoform 6) from seeds of *Saponaria officinalis* is presented. The fold typical of other plant toxins is conserved, despite some differences in the loop regions. The loop between strands β7 and β8 in the C-terminal region which spans over the active site cleft appears shorter in saporin, suggesting an easier access to the substrate. Furthermore we investigated the molecular interaction between saporin and the yeast ribosome by differential chemical modifications. A contact surface inside the C-terminal region of saporin has been identified. Structural comparison between saporin and other ribosome inactivating proteins reveals that this region is conserved and represents a peculiar motif involved in ribosome recognition.

Key words: Ribosome inactivating protein; Toxin; *N*-Glycosidase; Molecular recognition; *Saponaria officinalis*

1. Introduction

Ribosome inactivating proteins (RIPs) are a class of enzymes expressed by a wide array of plants, catalyzing specifically the cleavage of the *N*-glycosidic bond between the ribose and the adenine (A 4324 in the rat) within a universally conserved sequence of eukaryotic rRNA 28S [1]. The target adenine is involved in the binding of EF-1 and EF-2 to the ribosome, and therefore the toxin blocks the elongation step in protein translation. RIPs are classified into: type I RIPs, which are single chain proteins with molecular weights ranging from 26 to 31 kDa; and type II, made up by two disulfide-linked polypeptide chains, one essentially equivalent to a type I RIP, while the second is a lectin [2]. Some type I RIPs are also able to depurinate bacterial ribosomes by removing an adenine residue (A 2660 in *Escherichia coli*) which corresponds to A 4324 of eukaryotic (rat) rRNA. In both cases, the site of action is located in a highly conserved, purine-rich region (α-sarcin loop) of rRNA [3]. The catalytic activity of RIPs suggested [4] that a single molecule of the toxin may be sufficient to kill one cell. Nevertheless, their biological role is still unclear, although they were suggested to play a defensive role against viral or fungal infections in plants [5,6].

The catalytically active chain of RIPs is internalized by eukaryotic cells either by a natural vector such as the B-chain in type II RIPs, or by an artificial carrier for type I RIPs, leading as a final step to cell death by apoptosis [7]. Chemical cross-linking and protein engineering have been employed to synthesize chimeric proteins made of a type I RIP and a macromolecular carrier, often a monoclonal antibody directed against cancer cells. Some of these products are currently under clinical trial for the treatment of lymphomas [8,9].

Moreover, some of these toxins were shown to have a potential application for the treatment of viral infections, being able to inhibit HIV replication in lymphocytes [10,11]. Among type I RIPs, the three-dimensional structures of momordin (MOM), pokeweed antiviral protein (PAP), trychosantin and gelonin [12–15] have been determined. The crystal structure at 2.0 Å resolution of isoform 6 of saporin (SO6) purified from the seeds of *Saponaria officinalis*, a RIP widely used for the preparation of immunoconjugates, is reported below. In addition to a comparison of the 3D structure with that of other RIPs, we report chemical modification (foot-printing) experiments of the ribosome–saporin Michaelis complex; we identify three lysyl residues inside the C-terminal region (220–240) which map a structural motif, highly conserved throughout all RIPs, possibly involved in the enzyme–substrate molecular recognition mechanism.

2. Materials and methods

2.1. Purification, crystallization and data collection

Isoform SO6 of saporin was purified from the seeds of *S. officinalis* and crystallized as previously described [16]. Data were collected at room temperature on an R-AXIS II detector mounted on a rotating anode X-ray generator (50 kV × 100 mA). The number of collected oscillation images was 65, each corresponding to a rotation of 1.8° along the ϕ axis. The crystal-to-detector distance was set at 100 mm, which means a resolution of 2.0 Å at the edge of the detector. Diffraction data were processed and merged using DENZO and SCALEPACK [17]. The preliminary X-ray crystallographic analysis showed that crystals of SO6 belong to the tetragonal space group $P4_122$ or its enantiomorph $P4_322$.

2.2. Molecular replacement

Preliminary sequence alignment between SO6 and other RIPs of known structure led to a percentage identity ranging from 20 to 35%, the latter referring to the sequence of PAP. The relatively low sequence homology and the high symmetry of SO6 crystals make the molecular replacement (MR) approach a challenging task for solving the structure. Therefore, differently trimmed search models, in addition to very different parameters like Patterson integration radius, resolution limits, etc., were explored in the MR trials. Both ricin A chain (RTA, PDB code = 1rta) and PAP (PDB code = 1paf) were considered. Using these coordinates as starting points, we attempted the following search models: (i) the complete proteins, (ii) the polypeptide chains with all residues changed to alanines and (iii) models made by cutting out some long loops which have different structures among the various RIPs. The only acceptable solution was found using the whole protein atoms of PAP and performing the combined molecular replacement routine as implemented in the REPLACE package of pro-

*Corresponding author. Fax: (39)-6-4440062.
E-mail: tsernoglou@axcasp.caspur.it

PII: S0014-5793(00)01325-9

grams [18]. The search was carried out using reflections between 10.0 and 3.5 Å and placing the model inside a triclinic orthogonal cell of sides $a=b=c=100$ Å. Only Patterson densities inside a spherical volume with a radius of 25 Å were used in Patterson map superposition. The translational search was performed on the whole rotational map and not only on the highest peaks. Together with the correlation TF, a packing check criterion was applied: the minimum allowed distance between C_α belonging to symmetry-related molecules was set at 3.0 Å and all solutions with a number of violations above 8 were rejected. The best solution was found when the translational search was performed in the $P4_322$ space group with $R=48.6\%$ and only two bad contacts. The correctness of the solution was finally verified on the basis of the electron density map calculated after phase improvement procedures, including solvent flattening and histogram matching using the program DM [19]. With the model given by MR, a rigid body refinement was carried out at 2.5 Å resolution.

2.3. Refinement and quality of model

The final model obtained from the MR was refined with one cycle of simulated annealing refinement followed by positional refinement [20] with fixed *B*-factors at 20 Å^2. This procedure reduced the *R*-factor to 33.3% for data from 10 to 2.5 Å and a final R_{free} of 48.6%. The electron density map calculated after this stage showed a good agreement with the model on all the secondary structure elements, except that the random coils and the long C-terminal tail were hardly visible. So all the side chains of the non-conserved residues were changed to alanine and the residues in zones that did not fit the electron density were deleted from the model. Subsequently, with data from 15.0 to 2.0 Å, a procedure based on the combination of the programs REFMAC and ARP [19] was used, each cycle being followed by graphical inspections; after six cycles the *R*-factor dropped to 22.2% and the R_{free} to 27.0%. Thus it was possible to rebuild by hand with computer graphics the structure of the main chain and of all the side chains in their correct positions. At this stage 112 water molecules and one sulfate ion were added. Only waters whose density could be seen both in F_o-F_c and $2F_o-F_c$ maps were added, taking care to keep in the model only those with a *B*-factor below 60 Å^2 after refinement. Electron density map inspection and water addition were performed using the X-AUTOFIT and X-SOLVATE modules of the program QUANTA (Molecular Structure Inc.). This procedure allowed us to obtain a final model at 2.0 Å resolution with $R=18.2\%$ and $R_{free}=22.7\%$.

Table 1 gives the final refinement statistics and stereochemical parameters for the model of SO6.

2.4. Structure analysis

The geometrical quality of the model was analyzed using PROCHECK [19]. Most (92.8%) of the residues lie in the allowed regions in the Ramachandran plot and the remaining 7.2% in the additionally allowed regions. One non-conserved residue, Pro192, is in a *cis* conformation. Side chain conformational disorder was not observed. The average *B*-factor for all protein atoms (excluding H) is 22.6 Å^2, while the estimated value from a Wilson plot is 16.8 Å^2. From the structure solved at 2.0 Å it is possible to assign the correct amino acid sequence of SO6 from *S. officinalis* seeds [21]. The sequence deduced from direct chemical analysis presents some heterogeneity at positions 48 and 91, but from the density maps these residues are clearly assignable as aspartate and arginine, respectively. Moreover, it is confirmed that the corresponding sequence deduced from cDNA is that of the isoenzyme SO2 [22].

Structure superpositions with the related proteins were performed with the program INSIGHT (Molecular Structure Inc.). The refined coordinates have been deposited in the Protein Data Bank and the ID access code is 1QI7.

2.5. Differential chemical modification of SO6

Lysyl residues of SO6 were reacted with succinic anhydride in the presence (r-SO6) or absence (c-SO6) of yeast ribosomes (1:10 SO6: ribosome ratio) in 20 mM HEPES buffer pH 7.5 containing 50 mM KCl, 5 mM Mg acetate, 5 mM β-mercaptoethanol and 50% glycerol. The reaction was carried out for 2 h at 0°C, in order to slow down the enzymatic reaction catalyzed by SO6 and *freeze* the Michaelis complex. The reaction was stopped by addition of Tris and ribosomes were removed by ultracentrifugation. The supernatant containing SO6 was denatured by addition of 6 M guanidine HCl overnight, then extensively dialyzed against 20 mM bicarbonate (pH 8.4) and finally digested with trypsin. The proteolytic fragments, containing acetylated lysines in both r-SO6 and c-SO6, were separated by HPLC reverse phase chromatography (on a C4 Vydac column). Comparison of the chromatograms revealed the presence of peaks in the r-SO6 which were absent in c-SO6. These peaks were collected and sequenced by automated Edman degradation. Three unreacted lysyl residues, corresponding to positions 220, 226 and 234 in the sequence of SO6, were identified.

3. Results

3.1. Structure description and comparison with other RIPs

As shown in Fig. 1, SO6 is made up of two domains, the N-terminal domain which is predominantly β-stranded, and the C-terminal domain which is predominantly α-helical. The N-terminal domain is very similar to that of other RIPs. Six strands form a mixed β-sheet with four antiparallel β-strands in the center and those at the two edges which are parallel. The C-terminal domain contains eight α-helices with canonical geometry. Helices A and B are part of the cross-over connections between the parallel strands of the β-sheet. Helices E and F are contiguous in sequence and a single residue (Phe180) assumes a non-helical conformation, introducing a bend between the two helices (Fig. 1).

A structure superposition of SO6 with other RIPs is illustrated schematically in Fig. 2. Trichosantin and gelonin are not included in this analysis since the first is almost identical to MOM while the coordinates of the second are not yet available in the PDB. Insertions and deletions compared to PAP, MOM and RTA lie mainly in random coil regions. Most of the secondary structural elements are comparable, though the termini of the elements may be altered and the deviations are seen mainly in some loop regions particularly those between helix B and strand β6 (residues 101–109) and between helices C and D (residues 128–134). These loops are located on the surface.

The C-terminal region contains a two stranded antiparallel β-sheet element. The two strands are connected by a short loop whose length is variable among RIPs and particularly shorter (about three residues) in SO6 (Fig. 2).

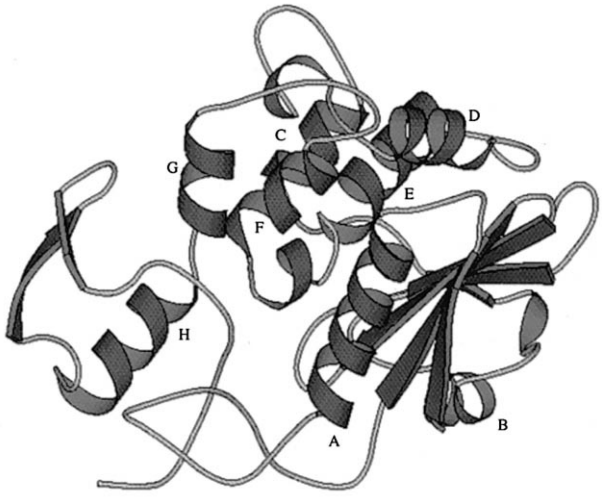

Fig. 1. A diagram of the folding of SO6. Letters A–H indicate the eight α-helices. The figure was prepared with the program Molscript.

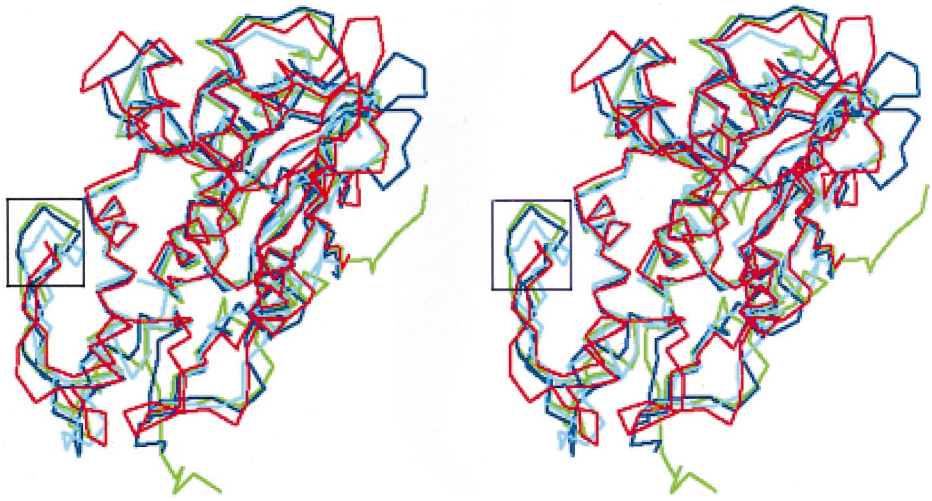

Fig. 2. Stereoview of the structures of SO6 (red), MOM (cyan), PAP (blue) and RTA (green), superimposed. The loop between strands β7 and β8 is outlined in the box.

The active site is conserved and almost perfectly superimposable to that of other RIPs, but the shorter loop present in the C-terminal region, covering the crevice of the active site, may be responsible for an increased accessibility to the substrate.

3.2. Differential chemical modification of SO6

To obtain some information on the surface of contact between SO6 and its substrate (the ribosome large subunit), we have employed a chemical foot-printing approach. The reaction of lysyl residues with succinic anhydride was employed in view of the large number of lysines (∼10% of residues) and their widespread distribution along the protein surface. The reaction was carried out in the presence or absence of yeast ribosomes to reveal the contact surface involved in the enzyme–substrate recognition mechanism [23].

After reaction with the anhydride, SO6 samples were digested with trypsin under denaturing conditions and the proteolytic fragments separated by RP-HPLC chromatography. Some differential peaks, identified upon comparing the chromatograms in the presence and absence of ribosomes, were analyzed by automated Edman sequence analysis. The corresponding proteolytic fragments (indicated in Fig. 3) revealed that three lysines (220, 226 and 234), which are close to one

```
MOM  (  1)            DVSFRLSGADPRSYGMFIKDLRN---ALPFREKVYNIPL
PAP  (  1)          VNTIIYNVGSTPISKYATFLNDLRN--EAKDPSLKCYGIPM
RTA  (  0)     MIFPKQYPIINFTTAGATVQSYTNFIRAVRG--RLTTGADVRHEIPV
SO6  (  1)          VTSITLDLVNPTAGQYSSFVDKIRNNVKDPNLKYGGTDIAV

MOM  ( 37)     L--LPSVSGAGRYLLMHLFNYDGKTITVALDVTNVYIMGY-----LA
PAP  ( 40)     L---PNTNTNPKYVLVELQGSNKKTITLMLRRNNLYVMGYSDPFETN
RTA  ( 45)     LPNRVGLPINQRFILVELSNHAELSVTLALDVTNAYVVGY-----RA
SO6  ( 42)     I-----GPPSKEKFLRINFQSSRGTVSLGLKRDNLYVVAYLAMDNTN

MOM  ( 77)     DTTSYFFNEPAAELASQYVFRDARRKI-----TLPYSGNYERLQIAA
PAP  ( 84)     KCRYHIFNDISGTERQDVETTLCPNALSRVSKNINFDSRYPTLESKA
RTA  ( 87)     GNSAYFFHPDNQE---DAEAITHLFTDVQNRYTFAFGGNYDRLEQLA
SO6  ( 84)     VNRAYYFKSEITS---AELTALFPEATTANQKALEYTEDYQSIEKNA

MOM  (119)     -----GKPREKIPIGLPALDSAISTLLHYDSTAA-----AGALLVLI
PAP  (131)     ----GVKSRSQVQLGIQIL--DSNIGKISGCMSFTEKTEAEFLLVAI
RTA  (131)     -----GNLRENIELGNGPLEEAISALYYYSTGGTQLPTLARSFIICI
SO6  (128)     QITQGDKSRKELGLGIDLL---LTFMEAVNKKARVVKNEARFLLIAI

MOM  (156)     QTAAEAARFKYIEQQIQER--AYRDEVPSLTAISLENSWSGLSKQIQ
PAP  (172)     QMVSEAARFKYIENQVKTN--FNRAFNPNPKVLNLQETWGKISTAI-
RTA  (173)     QMISEAARFQYIEGEMRTRIRYNRRSAPDPSVITLENSWGRLSTAI-
SO6  (172)     QMTAEVARFRYIQNLVTKN--FPNKFDSDNKVIQFEVSWRKISTAIY

MOM  (201)     LAQGNN-GIFRTPIVLVDNKGNRVQITNVTSKVVTSNIQLLLNTRNI
PAP  (216)     --HDAKNGVLPKPLELVDASGAKWIVLRVDEIKPDVALLNYVGGSCQT
RTA  (219)     --QESNQGAFASPIQLQRRNGSKFSVYDVSILIPIIALMVYRCAPPPS
SO6  (217)     --GDAKAGVFNKDYDFGF---GKVRQVKDLQMGLLMYLGKPK
```

Fig. 3. Sequence alignment based on structures. Residues conserved in all proteins are shown in bold. The underlined peptides correspond to the proteolytic fragments of saporin identified by HPLC analysis following differential chemical modification. The protected SO6 lysines (220, 226, 234) and corresponding residues in other RIPs are shown in italics.

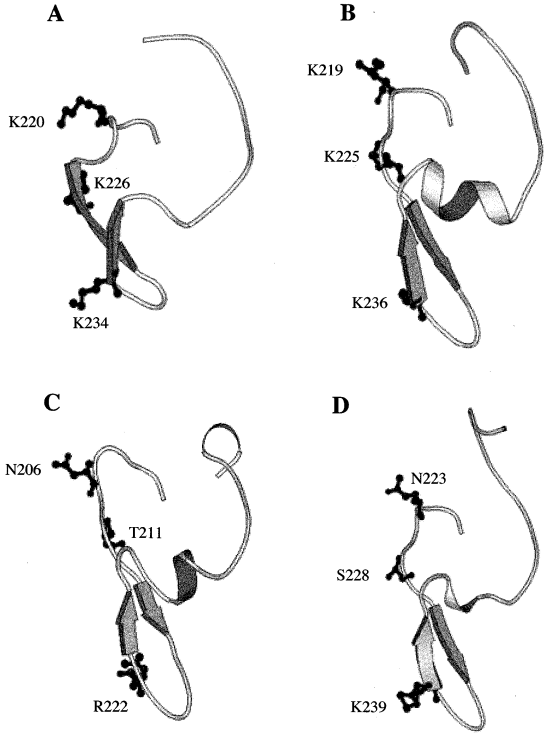

Fig. 4. The figure shows the C-terminal region of (A) SO6, (B) PAP, (C) MOM and (D) RTA. The residues putatively corresponding to the site of interaction with the ribosome are shown for each protein by ball and stick representation.

Table 1
Data collection and refinement

Effective resolution (Å)	2.0
Data completeness[a] (%)	98.5
R^{b}_{merge} (%)	10.9
Reflections with $I/3\sigma(I)$ (%)	82.0
Number of observations	210 203
Number of unique reflections	19 206
Space group	$P4_322$
Cell dimensions	$a=b=67.53$ Å
	$c=119.67$ Å
Refinement:	
number of atoms (hydrogen excluded)	2014
number of waters	112
number of sulfates	1
R-factor[c] (%)	18.2
R^{d}_{free} (%)	22.7
rmsd:	
bonds (Å)	0.012
angles (°)	2.24
Ramachandran (%):	
most favored	92.8
allowed (disallowed)	7.2 (0.0)
Average B-factor of protein atoms (Å^2)	22.63
Average B-factor of waters (Å^2)	35.34

[a]Completeness is the ratio of the number of observations to that of possible reflections.
[b]$R_{merge}=\Sigma_h\Sigma_i|I(h)_i-\langle I(h)\rangle|/\Sigma_h\Sigma_i I(h)_i$.
[c]R-factor $=\Sigma_h|F(h)_{calc}-F(h)_{obs}|/\Sigma_h F(h)_{obs}$.
[d]R_{free}: based on 10% reflections not used in refinement.

another in the C-terminal region of SO6, were protected: these three residues (Fig. 4) possibly map some of the contact area between SO6 and the ribosome. The structure-based alignment shows that positively charged or polar residues are located in the corresponding positions of PAP, MOM and RTA. In particular Lys220 in SO6 corresponds to Lys219 in PAP, Asn223 in RTA and Asn206 in MOM. Lys226 in SO6 corresponds to Lys225 in PAP, Ser228 in RTA and Thr211 in MOM. Finally Lys234 in SO6 corresponds to Lys236 in PAP, Lys239 in RTA and Arg222 in MOM (Fig. 3).

4. Discussion

Since the overall three-dimensional structure of SO6 has the fold typical of other RIPs, we have focused our attention on the catalytic site and on the C-terminal region putatively implicated in the molecular recognition of the substrate.

The active site residues Glu176, Arg179 and Trp208 are completely superimposable on those of other RIPs, while Tyr72, shown to be responsible for the interaction with the target adenine, assumes different side chain conformations among all analyzed RIPs. This may be accounted for by the role attributed to this residue which has been hypothesized to change its side chain conformation in allowing the substrate to enter and the hydrolysis product to leave the active site [24]. A more evident difference lies in residue Val206 whose topological position is occupied by asparagine in both MOM and RTA and by glutamate in PAP. The RNA–substrate loop, whose structure was determined by NMR [25] once modeled in the active side of MOM, shows that residue Asn190 plays a special role in the interaction with both the phosphate group and the ribose of G4323, thus contributing to the correct positioning with respect to the two catalytic residues [24]. This interaction cannot be supposed to occur both in SO6 and in PAP, even though no substantial loss of activity is observed [26]. The most striking difference lies in the loop between strands β7 and β8 which is shorter in SO6 than in all other RIPs (Fig. 2) and, being located just beyond the active site cleft, may control the accessibility to the substrate. This observation correlates well with the reported activity of SO6 which has been shown to hydrolyze adenosines other than the target, both in the rRNA and in superhelical DNA [27].

The interaction at the macromolecular level with the ribosome has been explored by differential chemical modification of lysyl residues of SO6: this technique revealed the presence of at least one region in the toxin putatively interacting with the ribosome. The structural motif of this region is peculiar and highly conserved among the analyzed RIPs. Moreover the three identified lysines (220, 226, 234) are either conserved or replaced by positively charged or polar residues. Given the limitations of this experimental procedure we can only speculate about the involvement of these residues in the molecular recognition of the ribosome. However, it should be outlined that deletion mutants of RTA in the corresponding C-terminal region (228–247) were found to be inactive [28].

Since the enzymatic activity of RIPs involves a gigantic substrate (the ribosome), a double step mechanism may be possibly envisaged for the molecular recognition, involving first interaction with ribosomal proteins and then attack of the r-RNA. We have previously demonstrated that SO6 can be cross-linked to yeast ribosomal proteins [29] and RTA was cross-linked to mammalian ribosomal proteins L9 and L10e [30]; furthermore, PAP has been recently shown to interact with *E. coli* L3 ribosomal protein [31]. In conclusion, it seems that RIPs possess a structural domain involved in overall recognition of the ribosomal surface and within a rather loose initial complex their active site can be correctly oriented towards the α-sarcin loop. Our data suggest for the first time that the C-terminal region may be involved in this interaction, although further experimental work is necessary to understand the role of lysines or other residues in the recognition and specificity.

Acknowledgements: The authors are extremely grateful to Dr. Liang Tong for valuable instruction in the use of the COMO procedure in the REPLACE suite, and to Dr. Doriano Lamba and Dr. Ken Johnson for helpful discussions and skillful advice in the early steps of MR and refinement procedures. Dr. Bruno Maras is gratefully acknowledged for providing the peptide analysis. Work partially supported by MURST (40% 1997 and PRIN Biologia Strutturale 1998 to D.T.) and by CNR (CTB CNR97.04161.04).

References

[1] Endo, Y. and Tsurugi, K. (1987) J. Biol. Chem. 262, 8128–8130.
[2] Barbieri, L., Battelli, M.G. and Stirpe, F. (1993) Biochim. Biophys. Acta 1154, 237–282.
[3] Hartley, M.R., Legname, G., Osborne, R., Chen, Z. and Lord, J.M. (1991) FEBS Lett. 290, 65–68.
[4] Olsnes, S. and Phil, A. (1982) in: Molecular Action of Toxins and Viruses (Cohen, P. and Van Heynegen, S., Eds.), pp. 81–105, Elsevier, Amsterdam.
[5] Lord, J.M., Hartley, M.R. and Roberts, L.M. (1991) Semin. Cell Biol. 2, 15–22.
[6] Leeds, R., Tommerup, H., Svendsen, I. and Mundy, J. (1991) J. Biol. Chem. 266, 1564–1573.
[7] Bolognesi, A., Tazzari, P.L., Olivieri, F., Polito, L., Falini, B. and Stirpe, F. (1996) Int. J. Cancer 68, 349–355.

[8] Falini, B., Terenzi, A., Liso, A., Flenghi, L., Solinas, A. and Pasqualucci, L. (1997) Cancer Surv. 30, 295–309.
[9] O'Tool, J.E., Esseltine, D., Lynch, I.S., Lambert, J.M. and Grossbard, M.L. (1998) Curr. Top. Microbiol. Immunol. 234, 57–61.
[10] Zarling, J.M., Moran, P.A., Haffar, O., Sias, J., Richman, D.D., Spina, C.A., Myers, D.E., Kuebalbeck, V., Leadbetter, J.A. and Uuckum, F.M. (1990) Nature 347, 92–95.
[11] Pan, L. and Levy, J.A. (1994) Curr. Ther. Res. 55, 718.
[12] Husain, J., Tickle, I.J. and Wood, S.P. (1994) FEBS Lett. 342, 154–158.
[13] Monzingo, A.F., Collins, E.J., Ernst, S.R., Irwin, J.D. and Robertus, J.D. (1993) J. Mol. Biol. 233, 705–715.
[14] Zhou, K., Fu, Z., Chen, M., Lin, Y. and Pan, K. (1994) Proteins 19, 4–13.
[15] Hosur, M.V., Nair, B., Satyamurthy, P., Misquith, S., Surolia, A. and Kannan, K.K. (1995) J. Mol. Biol. 250, 368–380.
[16] Savino, C., Federici, L., Brancaccio, A., Ippoliti, R., Lendaro, E. and Tsernoglou, D. (1998) Acta Crystallogr. D54, 636–638.
[17] Otwinoski, Z. and Minor, W. (1997) Methods Enzymol. 276, 307–326.
[18] Tong, L. (1996) Acta Crystallogr. A52, 782–784.
[19] Collaborative Computing Project #4 (1994) Acta Crystallogr. D50, 760–763.
[20] Brunger, A.T. (1988) J. Mol. Biol. 203, 803–815.
[21] Maras, B., Ippoliti, R., De Luca, E., Lendaro, E., Bellelli, A., Barra, D., Bossa, F. and Brunori, M. (1990) Biochem. Int. 21, 831–838.
[22] Barthelemy, I., Martineau, D., Ong, M., Matsunami, R., Ling, N., Benatti, L., Cavallaro, U., Soria, M. and Lappi, D. (1993) J. Biol. Chem. 268, 6541–6548.
[23] Rieder and Bosshard (1980) J. Biol. Chem. 255, 4732–4739.
[24] Ren, J., Wang, Y., Dong, Y. and Stuart, D.I. (1994) Structure 2, 7–14.
[25] Szewczak, A.A., Moore, P.B., Chang, Y.L. and Wool, D. (1993) Proc. Natl. Acad. Sci. USA 90, 9581–9585.
[26] Barbieri, L., Battelli, M.G. and Stirpe, F. (1993) Biochim. Biophys. Acta 1154, 237–282.
[27] Barbieri, L., Ferreras, J.M., Barraco, A., Ricci, P. and Stirpe, F. (1992) Biochem. J. 286, 1–4.
[28] Kitaoka, Y. (1998) Eur. J. Biochem. 257, 255–262.
[29] Ippoliti, R., Lendaro, E., Bellelli, A. and Brunori, M. (1992) FEBS Lett. 342, 154–158.
[30] Valter, C.A., Bartle, L.M., Leszyk, J.D., Lambert, J.M. and Goldmacher (1995) J. Biol. Chem. 270, 12933–12940.
[31] Hudav, K., Dinman, J.D. and Tumer, N.E. (1999) J. Biol. Chem. 274, 3859–3864.